ISSN 0001-4370, Oceanology, 2017, Vol. 57, No. 4, pp. 469–477. © Pleiades Publishing, Inc., 2017.
Original Russian Text © K.P. Silvestrova, A.G. Zatsepin, S.A. Myslenkov, 2017, published in Okeanologiya, 2017, Vol. 57, No. 4, pp. 521–530.

MARINE PHYSICS

Coastal Upwelling in the Gelendzhik Area of the Black Sea: Effect of Wind and Dynamics

K. P. Silvestrova[a, *], A. G. Zatsepin[a], and S. A. Myslenkov[b]

[a] *Shirshov Institute of Oceanology, Russian Academy of Sciences, Moscow, Russia*

[b] *Moscow State University, Faculty of Geography, Moscow, Russia*

**e-mail: ksberry@mail.ru*

Received November 21, 2016; in final form, December 6, 2016

Abstract—Long series data of a thermistor chain in the Black Sea coastal zone near Gelendzhik were analyzed. A thermistor chain installed 1 km offshore and at a depth of 22 m. There are full and incomplete upwelling events observed. The study of upwelling genesis based on: wind speed data from the NCEP/CFSR reanalysis and Gelendzhik weather station, velocity and direction of coastal currents measured by ADCP profiler moored on the bottom near the thermistor chain. Over the whole observation period (warm seasons of 2013–2015), more than 40 events of upwelling were registered four of them were full upwellings, when presence of under-thermocline water was observed near the sea surface. For every upwelling event, conditions prior to the changes in thermic structure, were analyzed. It is found that full upwelling generally occur under synergistic wind and current forcing. Fairly strong forcing of one of these factors is sufficient for partial upwelling to occur.

DOI: 10.1134/S0001437017040178

INTRODUCTION

Upwelling in Black Sea coastal zones is a fairly common event [1, 4, 8, 11]. It is generally related to wind forcing. In the Northern Hemisphere, coastal Ekman upwelling is caused by wind that blows along the coast when the coast is to the left of the wind. Integrated Ekman transport in the upper mixed layer (UML) is directed offshore, which leads to a compensational ascent of deeper and, generally, colder water, which sometimes reach the sea surface [5, 18]. Such an event is termed full upwelling. If cold water upwell but do not reach the sea surface, this is termed incomplete (partial) upwelling.

Coastal upwelling may also be caused by coastal currents of the same direction as the wind generating upwelling. In the northeastern part of the Black Sea, such a current is directed to the southeast [8]. In the Black Sea, the coastal current of this direction could be driven by mesoscale or submesoscale anticyclonic eddies, which are not directly related to wind forcing [3, 7, 11–13]. When the upwelling wind and current act together, they should intensify water ascent, which, in particular, is confirmed by the results of this study.

In this study, long series data of thermistor chain are analyzed. This thermochain moored 1 km offshore at a depth of 22 m in the Black Sea coastal zone near Gelendzhik. Full and incomplete upwelling events were identified. Wind speed reanalysis data, weather station data and current velocity data from an acoustic Doppler current profiler (ADCP), moored near the thermochain, were used to unveil driving factors of the observed events of upwelling.

DATA AND METHODS

In July 2012, a thermistor chain consisting of 17 temperature-sensing elements were deployed on a moored station with subsurface buoyancy 1 km offshore at a depth of 22 m. This point located at the satellite-covered hydrophysical test site of the Shirshov Institute of Oceanology, Russian Academy of Sciences [10] across from the Golubaya Bay (Gelendzhik). The sensors were placed on a wire at an equal distance (0.8 m) between them in the 6–20 m depth range. The sampling rate of the sensors was 30–60 s and their accuracy was ±0.05°C. Data from RDI WH Sentinel 600 kHz ADCP, which measured current velocity profiles every 30 s, available since 2013. The vertical resolution of the data is 0.5 m, in accordance with the ADCP cells. Table 1 lists the operating periods of the instruments.

For subsequent analysis, the original datasets were smoothed and the time series of the vertical distributions of water temperature, current speed and direction were plotted. Visualization of these datasets made it possible to delineate upwelling and downwelling events, as well as analyze the related wind and current parameters.

Wind forcing was calculated using the NCEP Climate Forecast System Reanalysis high-resolution dataset. The spatial resolution of the reanalysis data is ~0.2°, and the time step is 1 h [17]. The point of the

Table 1. Measurement periods of water temperature and current characteristics

Year	ADCP	Thermistor chain
2013	3 July–8 July 13 July–10 August 20 August–12 September 20 September–26 December	25 June–10 August 19 August–31 December
2014	6 May–15 May 30 May–9 June 18 June–20 June 3 July–8 July 11 July–19 July 24 July–1 August 5 August–23 August 25 August–26 October	21 February–10 April 6 May–15 May 30 May–11 June 18 June–20 June 1 July–8 July 11 July–1 August 4 August–24 September 25 September–31 December
2015	1 January–16 May 25 May–11 June 13 June–19 June 9 July–31 July 7 August–20 August 24 August–11 September 15 September–9 October	1 January–27 January 30 January–16 May 25 May–11 June June–19 June 9 July–9 October 13 October–31 December

reanalysis grid closest (~10 km) to the location of the thermistor chain and ADCP was picked. Data from the Gelendzhik weather station with 3-h temporal resolution were also used. To calculate the correlation coefficients (K) between wind forcing and water temperature, the initial temperature data were interpolated to 3-h time steps of weather observations and current velocity measurements were averaged.

The coordinate system was rotated 50° counterclockwise. Hence, positive velocity values correspond to the alongshore northwest current and southeast wind. This rotation angle was chosen in accordance with approximate orientation of the coast line in the study region.

Additionally, to reveal upwelling in the periods when the thermistor chain was not operational, water temperature measurements at the Golubaya Bay pier were used. Temperature was measured from the sea surface to 6 m depth in the summer months (June–July) during student field-works of the Oceanology Department, Faculty of Geography, Lomonosov Moscow State University. Daily measurements were performed at 09:00, 12:00, and 15:00 GMT using SISplus 1000 and CastAway CTDs [2].

RESULTS

During 2013–2015, in the warm period of year, more than 40 upwelling events were observed. Among them, four cases were full upwellings when the presence of deep water with temperatures of 10–12°C were recorded by the upper sensor of the thermochain at a depth of 6 m. Itis found that full upwelling events do not occur every year and are often associated with early summer (May–June) or autumn (September–October), which is confirmed by other studies [4, 14]. Partial upwelling is observed more often, at least twice a month. The duration of the full upwelling–downwelling cycle varies from several days to 1.5 weeks, which is also shown in [11, 14, 16].

During incomplete upwelling, no significant temperature changes were recorded by the upper thermosensor. At lower depths (more than 10 m), however, sensors registered presence of water that has temperature 2–10°C lower than near-surface water. This temperature difference depends on the intensity of the upwelling event. The temperature decrease is caused by the ascent of the seasonal thermocline, its upper boundary reaches the sea surface during a full upwelling event. An example of partial upwelling in July 2015 is shown in Fig. 1. This event was caused by intense wind forcing (the Ekman upwelling criterion, which is described below, is less than –1), but the presence of a thick UML and absence of the strong southeastern current hindered the ascent of deep waters to the depth of the upper sensor of the thermistor chain.

During downwelling, the upper boundary of the thermocline often descends to more than 20 m (the depth of the last sensor in the thermochain) and thermal stratification disappears in the whole water column. Such short-term change of the hydrologic structure is accompanied by intense water advection, as well as vertical and horizontal water mixing. These processes seem to significantly influence the hydrochemical structure of water and flows of nutrients and pollutants, which leads to a change in the functional conditions of the coastal ecosystem [6].

As mentioned above, upwelling and downwelling in sea coastal zones are caused by wind forcing, alongshore currents or both. To reveal the relationship between wind speed, current speed, and sea temperature, the correlation coefficients for these parameters were calculated (Fig. 2). The longshore component of the wind speed, longshore component of the current speed at a depth of 7 m, and sea temperature at depths of 6, 9.2, 13.2, and 19 m were used. A small correlation coefficient was found between temperature and wind speed ($K < 0.3$), as well as between temperature and current speed ($K < 0.4$). When the correlation coefficients were calculated for periods of full upwelling, a considerable correlation between temperature and wind speed was found, which reaches its maximum ($K > 0.7$) when the temperature records are shifted 27–33 h forward. The response of the near surface temperature to a wind speed change occurs later than the temperature response at lower depths, which is natural for upwelling events. In the same cases, the correlation between temperature and the speed of the longshore current is higher than between temperature and wind speed, reaching $K > 0.8$ for the same time shift.

For incomplete upwelling events, the correlation coefficients between sea temperature and wind speed were low ($K < 0.5$) for any temporal shifts. At the same time, the correlation with current speed was found to be high ($K \approx 0.8$) for lower depths, where rising of the isotherm was observed. These calculations show that,

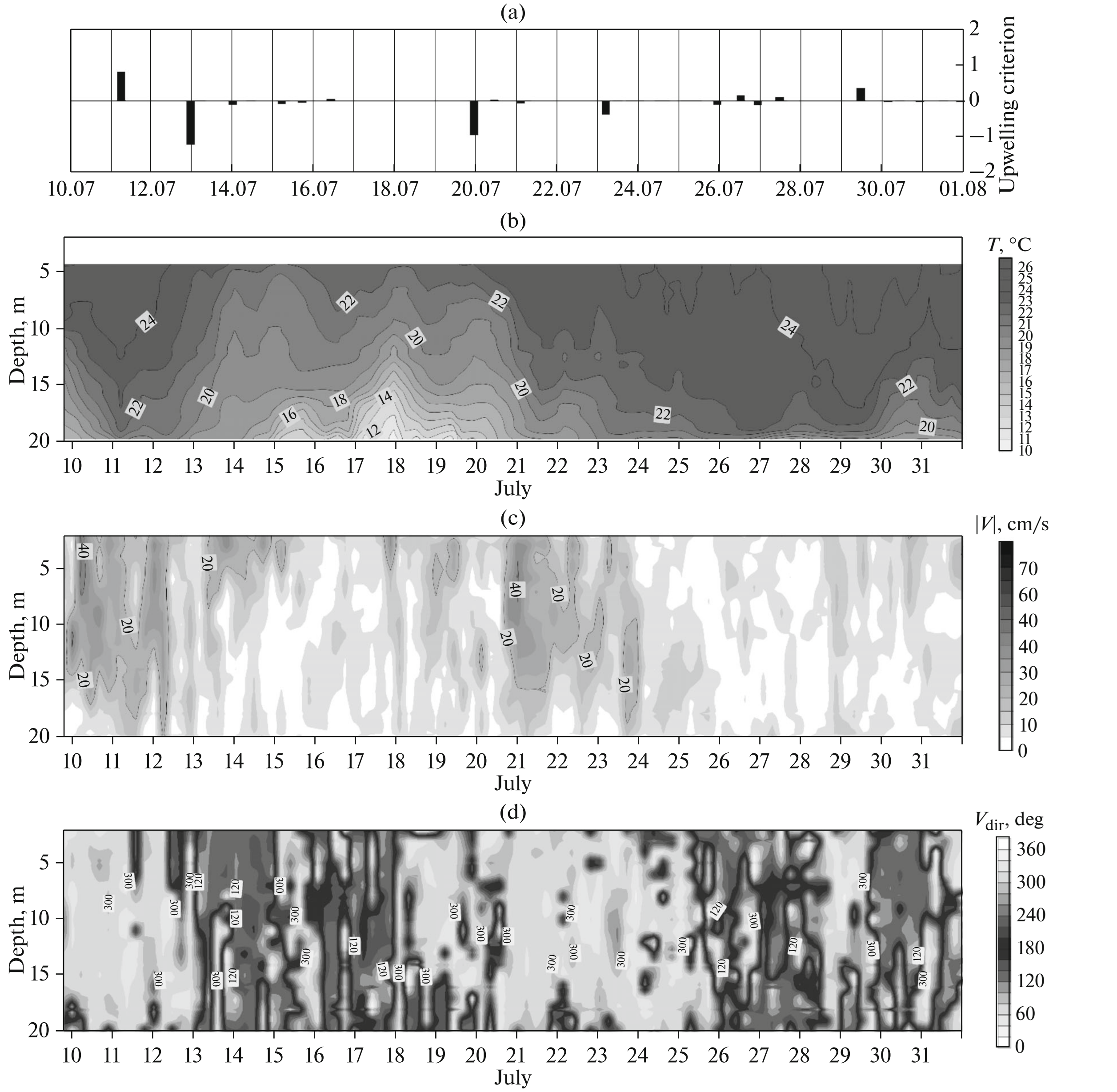

Fig. 1. (a) Upwelling criterion R_u. Vertical distributions of (b) temperature, (c) current velocity and (d) direction at analyzed point in July 2015, when incomplete upwelling was observed.

unlike full upwelling, partial upwelling is not wind forced, but related to the dynamics of coastal currents.

To estimate the possibility of a full upwelling event forced by the wind (Ekman) factor, the following criterion was suggested in [11]:

$$R_u = \tau_y t / f \rho_w H R_d = u_*^2\, t/(g' H^3)^{1/2} < -1. \quad (1)$$

Here, τ_y is the longshore component of wind stress, t is duration of quasi-stationary forcing of the upwelling wind, f is Coriolis parameter, ρ_w is sea water density, H is thickness of UML, $R_d = (\Delta\rho g H/\rho_w)^{0.5}/f$ is the local baroclinic Rossby deformation radius, $g' = g\Delta\rho/\rho_w$ is reduced acceleration due to gravity, $\Delta\rho$ is the difference between water densities in the upper (above thermocline) and lower (under thermocline) layers, and $u_* = (\tau_y/\rho_w)^{1/2}$ is the dynamic friction velocity in water.

The R_u values were calculated for all upwelling events. The lower layer was defined as a layer with temperature of 10°C. The average climatological values of the water density and temperature, thickness of UML were used. The criterion $R_u < -1$ for three full upwelling events out of four recorded. As found, the typical duration of the upwelling wind is more than two days. This means that continuous northwestern wind forcing is needed for development of full upwelling in this region, but such conditions occur very rarely. Thus, Eq. (1)

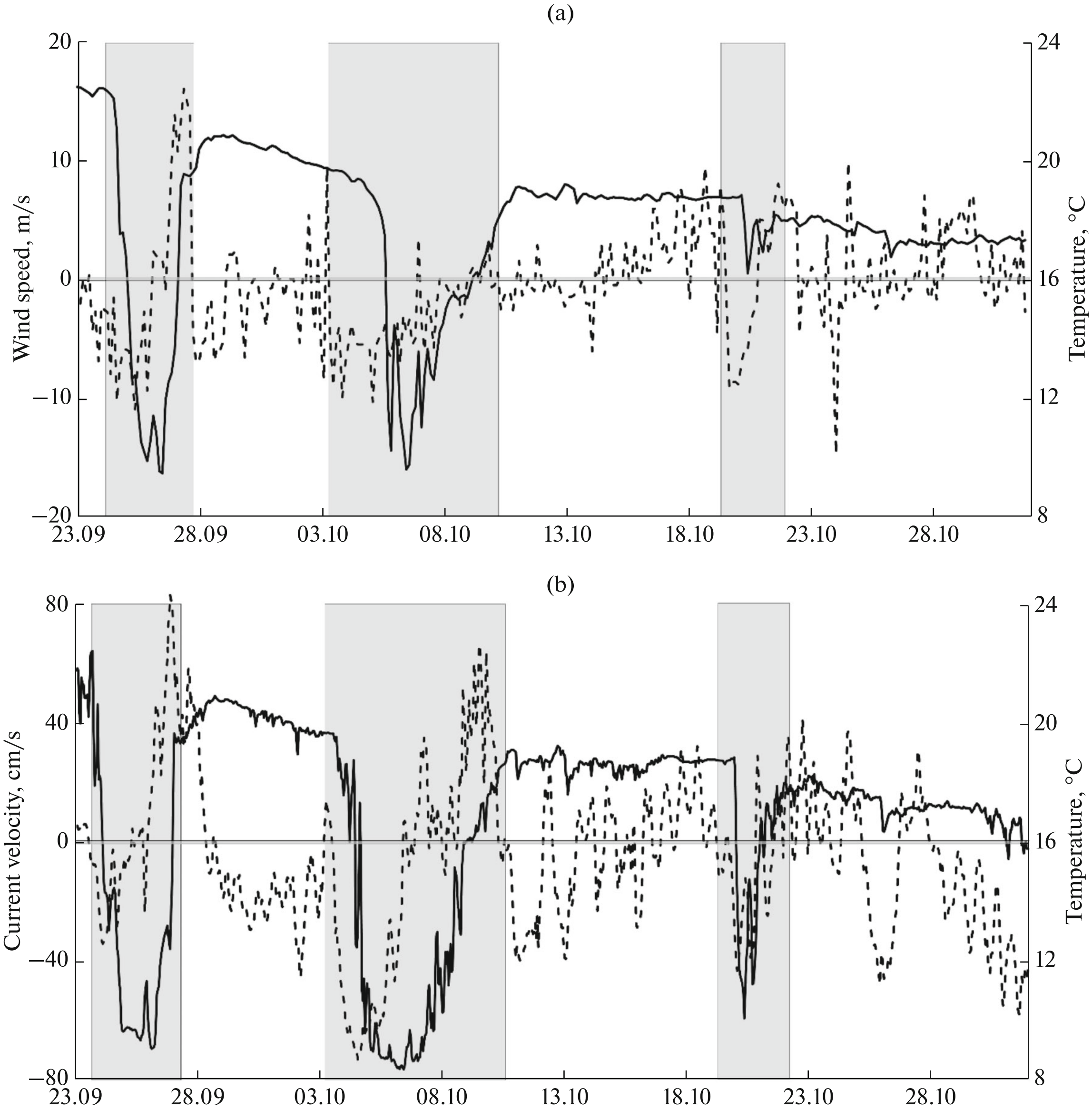

Fig. 2. (a) Water temperature at depth of 9 m (solid line) and longshore component of wind speed (dashed line) in September–October 2013. (b) Water temperature at depth of 19 m (solid line) and longshore component of current velocity (dashed line) in September–October 2013. Upwelling periods are shaded.

provides representative diagnostic or prognostic assessments of the full Ekman upwelling probability based on climatological thermocline temperature variation and UML thickness data, observed (or forecasted) wind.

Main characteristics of full and incomplete upwelling presented in Table 2, where several types are identified according to the values of the R_u criterion and water dynamics data. There are 40% of the recorded

Table 2. Upwelling characteristics

Ekman upwelling criterion R_u	Direction and velocity of current	Temperature change at 18 m depth	% of total
Less than –0.5 (incl. less than –1)	SE, >30 cm/s	>7° C	40% (incl. 3 cases of intensive upwelling)
From –0.5 to –0.2	SE, about 20 cm/s	4–7° C	22%
From –0.2 to 0.1	Alternating sign	3–7° C	14%
From –0.2 to 0.1	SE, 20–30 cm/s	1–5° C	11%
From –0.2 to 0.1	SE, 30–50 cm/s	3–4° C	9%
Less than –0.6	10–20 cm/s	2–3° C	4%

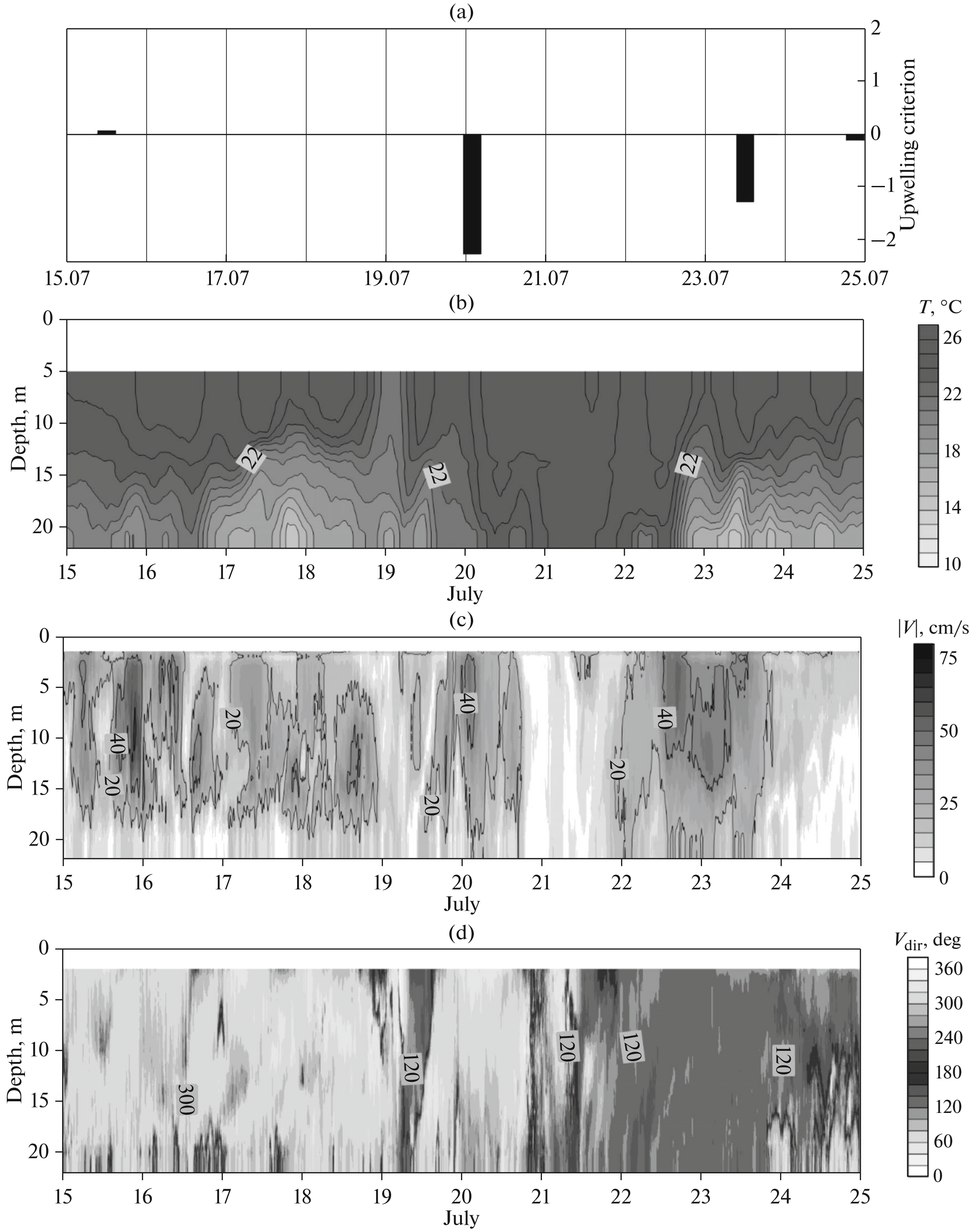

Fig. 3. (a) Upwelling criterion. Vertical distributions of (b) temperature, (c) current velocity and (d) direction at analyzed point from July 15 to 25, 2013.

events, including three cases of full upwelling, when high absolute values of the R_u criterion and strong southeastern currents were observed. The upwelling criterion was from –0.5 to –0.2 for 22% of events, which were characterized by continuous wind forcing with moderate southeastern current. Only 14% of cases (when temperature changes at the lower sensor indicate vertical movements of the thermocline) related to the turn of the alongshore current, which could be explained by the passage of submesoscale eddies or topographic waves.

In some situations (11% of cases), ascent of thermocline waters occurred without wind forcing, but with a strong southeastern current.

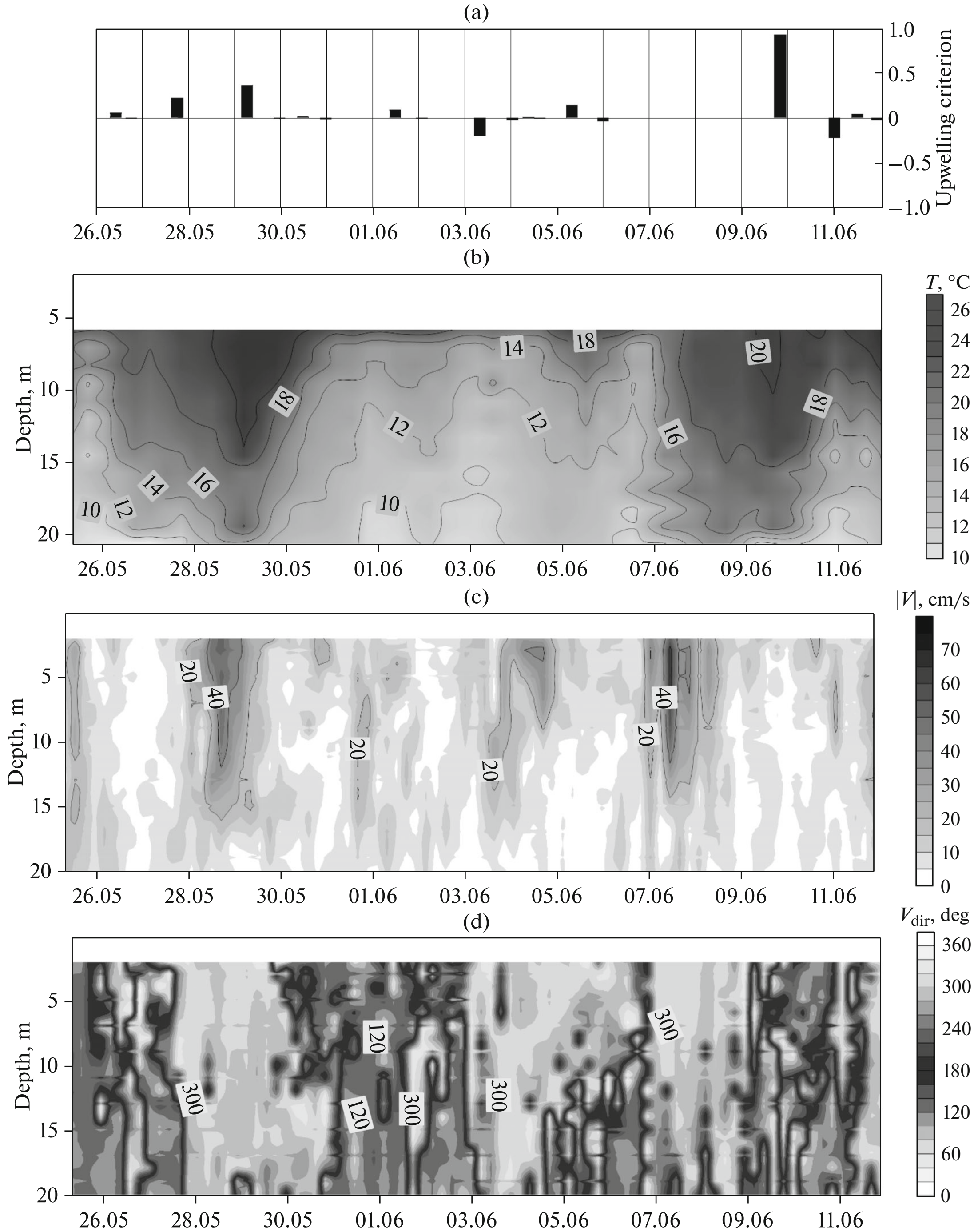

Fig. 4 (a) Upwelling criterion. Vertical distributions of (b) temperature, (c) current velocity and (d) direction at analyzed point from 25 May to 12 June 2015.

Rarest are the cases when partial upwelling developed only due to the wind forcing ($R_u < -0.6$) with low current speeds. There are 9% of cases of upwelling occurrence with low current speeds and low absolute values of the Ekman upwelling criterion (from 0.1 to –0.2). Such partial upwelling is unsustainable and recorded after upwelling events with the above-mentioned features.

However, in some cases when criterion (1) was enough, there was no full upwelling observed (Fig. 3). One possible reason is discrepancy between the mean climatological UML thickness and its real value [15]. Due to considerable short-term (several days) variability in the magnitude and direction of the longshore current [3] the UML also varies. The next logical step of this research is estimation of the UML thickness variability and its correlation with the longshore current speed. However, a shallow depth (22 m) of moored station does not allow to estimate the UML

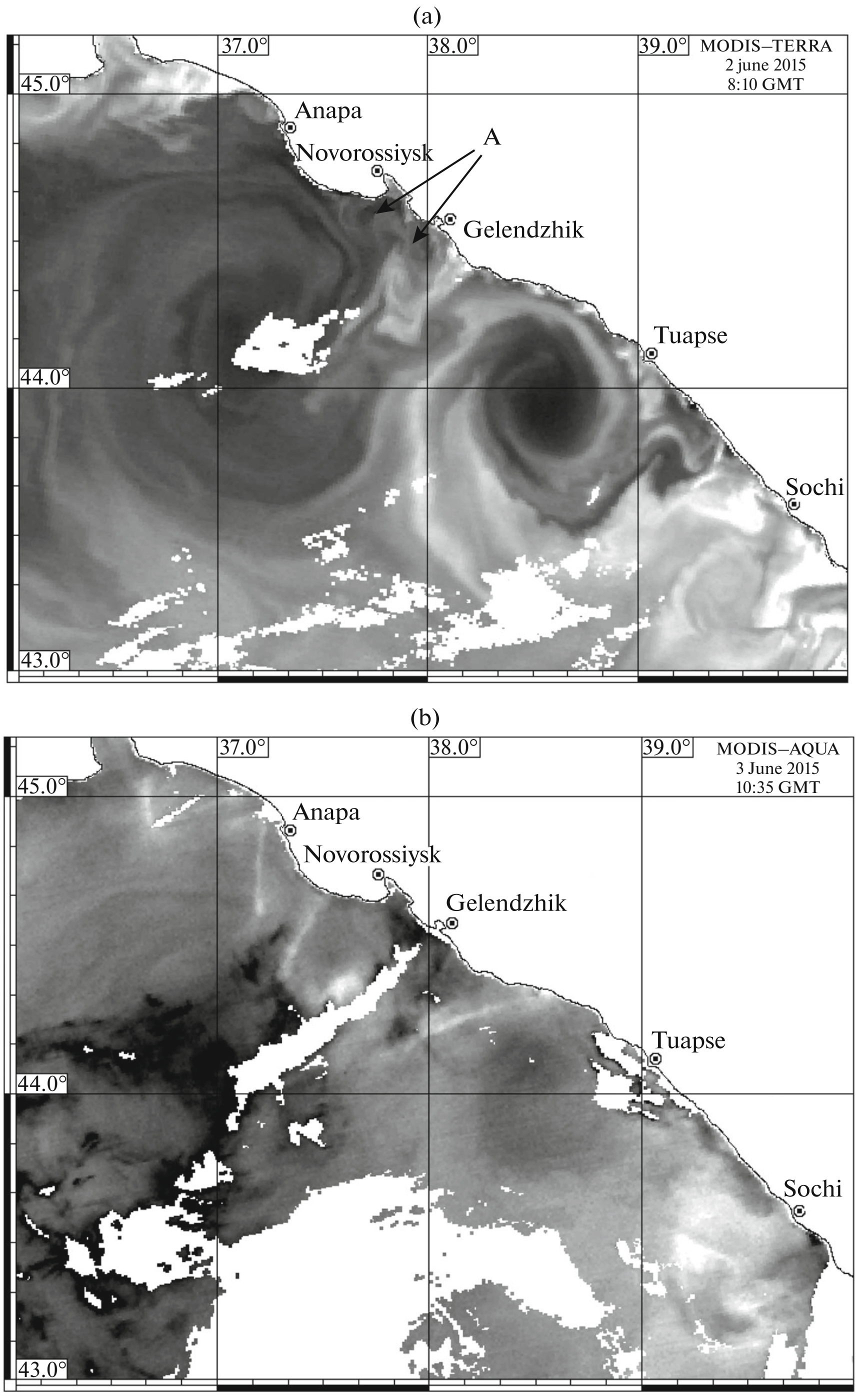

Fig. 5. Satellite images of northeastern part of the Black Sea. (a) MODIS-Terra optical image for 08:10 GMT on June 2, 2015; arrows indicate two submesoscale anticyclonic eddies (A) in Gelendzhik–Novorossiysk coastal zone, which advect waters in southeast direction and produce upwelling; (b) MODIS-Aqua sea surface temperature (SST) for 10:25 GMT on June 3, 2015; decrease in SST by 2–3° C is observed (dark tones) in Gelendzhik–Novorossiysk region, which is related to upwelling in A.

thickness, because in many situations, particularly those related to downwelling events, the UML extends to the bottom. To estimate the variability range of the UML, it is necessary to move the measurement point to deeper areas, which is planned in the near future.

A considerable increase of the UML thickness compared to the average climatological values is observed in the presence of a northwestern current, which causes deepening of the thermocline in the direction of the coast due to geostrophic adjustment [6]. Such situation was observed in July 2013 (Fig. 3), when full upwelling didn't occur even under strong and continuous upwelling wind.

A special case is the full upwelling event recorded from 29 May to 7 June, 2015 (Fig. 4). This upwelling developed in the absence of both northwestern wind and strong southwestern current. Satellite images of the sea surface (Fig. 5) provide an explanation of this phenomenon. Figure 5a shows an optical image obtained by the MODIS-Terra scanner at 08:10 GMT on June 2, 2015, which captured the northeastern part of the Black Sea. The arrows indicate two submesoscale anticyclonic eddies in the Gelendzhik–Novorossiysk coastal zone that produce upwelling and longshore advection of colder water in the southeast direction. Due to this advection, cold water reaches the point where the station with the ADCP and thermistor chain is moored. Figure 5b shows sea surface temperature field (SST) of the same part of the Black Sea obtained by the MODIS-Terra scaner at 10:25 GMT on June 3, 2015. As observed, in the area of submesoscale eddies, the SST values are lower (by approximately 2–3°C) compared to the surrounding waters. The absence of an obvious current at the point of the site means that, apparently, this point was located on the periphery of the anticyclonic eddy, which was reached by upwelling waters due to longshore advection. Upwelling events caused by submesoscale eddies were described before in [9], and their presence should be noted when analyzing thermocline water upwelling events in the Black Sea coastal zone.

Some incomplete upwelling events are also presumably caused by relaxation (recovery of thermocline location after downwelling). However, clear separation of relaxation and upwelling is challenging, because these events constantly replace each other and there is ambiguity in choosing the thermocline depth.

CONCLUSIONS

Development of full coastal upwelling in the northeastern part of the Black Sea is generally preceded by a sustained and continuous (more than two days) northwestern wind. Initialization of the process is related to the intrusion of cold under-thermocline waters to the near-bottom layer, which gradually ascend to the sea surface. Development of full upwelling is facilitated by the presence of a southeastern coastal current. Full upwelling usually occurs in the presence of two factors, i.e., a northwestern wind and southeastern current. When the wind forcing ends, the upwelling relaxes. The relaxation speed significantly increases when the longshore current turns to the northwest. Under such conditions, downwelling develops.

The criterion for full Ekman upwelling (see Eq. (1)) is a useful predictor of its occurrence. However, neglecting the influence of the water dynamics lowers its credibility.

At the measurement site (depth of 22 m), oscillations in the direction of the longshore current cause vertical oscillations of the upper boundary of the thermocline with an amplitude of 10 m or more. These oscillations are one of the main reasons for the frequent occurrence (two to three times a month) of incomplete upwelling. For incomplete upwelling it is sufficient presence of an intense southeastern current; the role of the wind is not important in this case.

The possibility of local ascent of cold waters at the cores of submesoscale eddies and consequent advection of these waters by longshore currents should be considered, when coastal upwelling events analyzed.

ACKNOWLEDGMENTS

The authors are grateful to D.M. Soloviev for kindly providing the satellite images.

Instrument installation and obtaining of measurement data were supported by the Russian Science Foundation, (project no. 14-17-00382). Data processing and analysis was supported by the Russian Foundation for Basic Research (project no. 14-05-00159).

REFERENCES

1. V. S. Arkhipkin, Candidate's Dissertation in Geography (Moscow, 1966).
2. V. S. Arkhipkin, S. A. Dobrolyubov, S. S. Mukhametov, et al., "Extreme rainwater in the Ashamba River basin and its influence on the seabed relief and the seawater structure in the region of Gelendzhik," Vestn. Mosk. Univ., Ser. 5. Geogr., No. 3, 27–34 (2013).
3. A. S. Blatov and V. S. Tuzhilkin, "Medium-scale eddies and synoptic variability in the World Ocean," Itogi Nauki Tekh., Ser.: Okeanol. **8**, (1990).
4. R. V. Borovskaya, B. N. Panov, E. O. Spiridonova, et al., "Coastal Black Sea upwelling and interannual intensity dynamics," in *Ecological Safety of the Coastal and Shelf Zones and Complex Use of Shelf Resources* (Sevastopol, 2005), No. 12, pp. 42–48.
5. V. M. Zhurbas, I. S. Oh, and T. Park, "Role of the beta-effect in the decay of the alongshore baroclinic jet associated with transient coastal upwelling and downwelling: numerical experiments," Oceanology (Engl. Transl.) **46**, 170–177 (2006).
6. A. G. Zatsepin, D. N. Elkin, A. O. Korzh, S. B. Kuklev, O. I. Podymov, A. G. Ostrovskii, and D. M. Soloviev, "On influence of current variability in the deep Black Sea upon water dynamics of narrow North Caucasian continental shelf," Phys. Oceanogr. **3**, (3), 14–22 (2016).
7. A. G. Zatsepin, V. I. Baranov, A. A. Kondrashov, A. O. Korzh, V. V. Kremenetskiy, A. G. Ostrovskii, and D. M. Soloviev, "Submesoscale eddies at the Caucasus Black Sea shelf and the mechanisms of their generation," Oceanology (Engl. Transl.) **51**, 554–567 (2011).
8. A. G. Zatsepin, V. V. Kremenetskiy, S. V. Stanichnyi, and V. M. Burdyugov, "Wind-caused basin circulation and mesoscale dynamics of the Black Sea," in *Modern Dynamics of the Ocean and Atmosphere*, Ed. by A. V. Frolov and Yu. D. Resnyanskii (Triada, Moscow, 2010), pp. 347–368.
9. A. G. Zatsepin, A. G. Ostrovskii, V. V. Kremenetskiy, V. B. Piotukh, S. B. Kuklev, L. V. Moskalenko, O. I. Podymov, V. I. Baranov, A. O. Korzh, and S. V. Stanichny, "On the nature of short-period oscilla-

tions of the main Black Sea pycnocline, submesoscale eddies, and response of the marine environment to the catastrophic shower of 2012," Izv. Atmos. Ocean. Phys. **49**, 659–673 (2013).

10. A. G. Zatsepin, A. G. Ostrovskii, V. V. Kremenetskiy, S. S. Nizov, V. B. Piotukh, V. A. Soloviev, D. A. Shvoev, A. L. Tsibul'sky, S. B. Kuklev, O. N. Kukleva, L. V. Moskalenko, O. I. Podymov, V. I. Baranov, A. A. Kondrashov, A. O. Korzh, et al., "Subsatellite polygon for studying hydrophysical processes in the Black Sea shelf-slope zone," Izv. Atmos. Ocean. Phys. **50**, 13–25 (2014).
11. A. G. Zatsepin, K. P. Silvestrova, S. B. Kuklev, V. B. Piotoukh, and O. I. Podymov, "Observations of a cycle of intense coastal upwelling and downwelling at the research site of the Shirshov Institute of Oceanology in the Black Sea," Oceanology (Engl. Transl.) **56**, 188–199 (2016).
12. V. G. Krivosheya, L. V. Moskalenko, and V. B. Titov, "On the current regime over the shelf near the North Caucasian coast of the Black Sea," Oceanology (Engl. Transl.) **44**, 331–336 (2004).
13. K. P. Silvestrova, S. A. Myslenkov, A. G. Zatsepin, E. V. Krayushkin, V. I. Baranov, T. E. Samsonov, and S. B. Kuklev, "GPS-drifters for study of water dynamics in the Black Sea shelf zone," Oceanology (Engl. Transl.) **56**, 150–156 (2016).
14. A. A. Novikov and V. S. Tuzhilkin, "Seasonal and regional variations of synoptic anomalies of water temperature in the northeastern part of the coastal zone of Black Sea," Morsk. Gidrofiz. Zh., No. 1, 42–52 (2015).
15. O. I. Podymov and A. G. Zatsepin, "Seasonal anomalies of water salinity in the Gelendzhik region of the Black Sea according to shipborne monitoring data," Oceanology (Engl. Transl.) **56**, 342–354 (2016).
16. V. S. Tuzhilkin, V. S. Arkhipkin, S. A. Myslenkov, and T. V. Samborskii, "Synoptic thermohaline variability in the Russian coastal zone of the Black Sea," Vestn. Mosk. Univ., Ser. 5. Geogr., No. 6, 46–53 (2012).
17. S. Saha, S. Moorthi, X. Wu, et al., "The NCEP climate forecast system, version 2," J. Clim. **27**, 2185–2208 (2014). doi doi 10.1175/JCLI-D-12-00823.1
18. M. Tomczak and J.S Godfrey, *Regional Oceanography: an Introduction* (Pergamon, Oxford, 1994).

Translated by P. Golubkin